Tunnel Structural Inspection and Assessment using an Autonomous Robotic System

Elisabeth Menendez*, Juan G. Victores, Roberto Montero, Santiago Martínez, Carlos Balaguer

Robotics Lab research group within the Department of Systems Engineering and Automation at Universidad Carlos III de Madrid (UC3M)

Abstract

This paper presents the ROBO-SPECT European FP7 project, funded under the ICT-2013.2.2 programme on Robotics use cases & Accompanying measures, a robotized alternative to manual tunnel structural inspection and assessment of cracks and other defects. Physical developments include the design and implementation of a multi-degree-of-freedom robotic system, composed by a mobile vehicle, an extended crane, and a high precision robotic arm. A semi-supervised computer vision system to detect tunnel defects, and a ultrasonic sensor (US) robotic tool to measure width and depth of detected cracks have been also developed. An overview of defect detection methods, as well as the fundamental aspects of the project architecture and design, will be presented. In addition, the developed and implemented arm tip positioning algorithm for the US robotic tool shall be detailed. Finally, experimental evidence and details on validation in a real motorway tunnel with ongoing traffic will be provided.

Keywords:

Mechatronic Systems; Automation; Control of Robotic Systems; Design; Computer Vision; Tunnel; Inspection; Maintenance.

*Corresponding author

Email addresses: emenende@pa.uc3m.es (Elisabeth Menendez), jcgvicto@ing.uc3m.es (Juan G. Victores), romonter@pa.uc3m.es (Roberto Montero), scasa@ing.uc3m.es (Santiago Martínez), balaguer@ing.uc3m.es (Carlos Balaguer)

1. Introduction

The structural performance of tunnels is time-dependent because of the deterioration processes induced by natural and man-made impacts, changes in load criteria, or the simple effect of ageing. Therefore, inspection, assessment and maintenance are required to ensure that these constructions remain in safe condition and continue to provide reliable levels of service. Tunnels of all kinds, including water supply, metro, railway and road, have increased in both total length and number, and will continue to do so on a global scale. Some tunnels still in service were constructed over 50 years ago, and many have exceeded their intended design service life [1]. Only in Europe in 2002, the overall length for operational transportation tunnels had grown up to 15000 km [2].

Tunnel environments are characterized by dust, humidity, absence of natural light, and the existence of toxic substances among others. Inspection and maintenance are frequently performed by human operators in these unfriendly environments. Manual inspection processes are time-consuming, and must rely on expert trained operators. Additionally, human error tend to cause poor quality inspections.

An automated, cost-effective and exhaustive inspection of tunnels will improve short and long-term security, and increase productivity [3]. In this work, we present the integrated ROBO-SPECT system, which is a promising solution to the problems described above. This paper also describes the arm positioning algorithm for placing the Ultrasonic Sensors on detected cracks, followed by experimental evidence ranging from initial simulation and laboratory testings to demonstrations in motorway tunnels with ongoing traffic. Finally, results and conclusions are presented.

1.1. Tunnel Inspection Methods

The majority of tunnel linings use reinforced concrete and a significant number of them contain ceramic tiles and metal panels. According to SHRP 2 projects [4], several defects in tunnel linings are hidden from view, however this work focuses on the inspection of visible defects.

Figures 1 and 2 display the most common visible defects in tunnel lining, which are cracks, spalling and efflorescence.

- Cracks are linear fractures in the concrete caused by tensile forces exceeding the tensile strength of the concrete.
- Spalling is the detachment of hardened concrete that leave a roughly circular or oval depression.
- Efflorescence is a deposit of water-soluble calcium hydroxide that forms on the concrete surface.

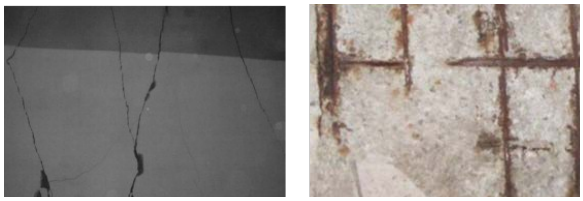

Figure 1: Crack observed in the lining of Longxi tunnel (left) [5] and concrete spalling with exposed reinforcing steel. (right) [1].

Figure 2: Moderate cracking and efflorescence on the underside of the liner [1].

In order to know if the structure is still safe without causing side effects, it is preferable to use non-destructive evaluation (NDE) methods [6]. NDE methods in structures can be classified in visual, strength-based, sonic and ultrasonic, magnetic, electrical, thermographic, radar electromagnetic, radiographic, and endoscopy methods.

- Visual inspection, performed by inspectors, is an essential precursor to any intended non-destructive test.

- Strength-based tests measure the surface hardness of materials and provide an estimation of surface compressive strength, uniformity and quality of the structure. Examples of hardness testers include the Windsor Probe [7] and the Schmidt Hammer [8].

- In sonic methods [9], also known as impact-echo tests, hammer impacts on the wall generates waves that are reflected at discontinuities in the material and a receiver records the signals. The depth of these discontinuities is determined by analyzing the frequency spectrum of the recorded signals.

- Ultrasonic methods [10] are normally based on velocity measurements of pulses generated by a piezoelectric transducer on the material. The pulse velocity depends on the composition and maturity of the structural material and its elastic properties.

- Magnetic methods [11] are important in corrosion control since they are used to determine the position of reinforcing bars. Examples of these methods are the Magnetic Flux Leakage method or the Magnetic Field Disturbance method.

- Electrical methods [12] based on electrical resistance are used to estimate corrosion rate for reinforced concrete.

- Thermographic methods [13] measure the thermal radiation emitted by the tunnel lining and allow a visual representation of the temperature distribution on the surface. The temperature on the surface represents the thermal flow through the surface, which in turn is influenced by the mechanical and/or hydraulic discontinuities of the structure. Consequently, thermal discontinuities on a surface reflect abnormalities within the underlying structure.

- Radar electromagnetic methods [14] have been widely used to detect defects in tunnels and other structures. The most used is the Ground-Penetrating Radar (GPR), which is based on the propagation of electromagnetic energy through materials of different dielectric properties.
- Radiographic methods [15], such as those based on X-rays, gamma radiation, or neutron rays, can penetrate structural materials and therefore can be used with inspection purposes. The amount of radiation absorbed by the material is dependent on density and thickness.

1.2. Robotic Systems for NDE Inspection of Concrete Structures

In recent years, the development of concrete inspection and maintenance robotic systems has been an area of increasing research interest. These robots are expected to provide exhaustive inspections with high productivity and increased safety.

Vehicle-based systems have been developed for off-line detection of defects on the tunnel lining. A mobile robot for crack detection via computer vision algorithms is reported in [16]. A similar system to detect deformations by fusing cameras and ultrasonic sensors data is developed [17]. Suda et al. present a system composed by a truck and a robotic arm equipped with a multi-hammer that generates impact sounds to find cavities and exfoliation areas [18]. A bridge inspection system using machine vision techniques is reported in [19]. TUNCONSTRUCT teleoperated system [20] performs a set automated maintenance task on the tunnel lining: superficial preparation, fissure injection and Fiber Reinforced Polymer (FRP) composite adhesion in the tunnel.

The previous systems do not allow remote inspection and need to be partially or completely teleoperated. An autonomous mobile robot is developed for bridge deck data collection, inspection and analysis [21, 22]. NDE data gathered with this system for crack, delamination and corrosion detection is evaluated in [23, 24]. Difference to all of the above-mentioned works, this paper focuses on the development of a robotic system to perform automated tunnel inspection using NDE methods and data collection.

2. The ROBO-SPECT European Project

ROBO-SPECT is a research project co-funded by the European Commission under the 7th Framework Programme (FP7) ICT-2013.2.2 on Robotics use cases & Accompanying measures, running between October 2013 and October 2016, composed by a Consortium of 12 partners, coordinated by the Institute of Communication and Computer Systems (ICCS). The objective of ROBO-SPECT is to provide an automated, faster and reliable tunnel inspection of cracks and other defects, and assessment solutions that can combine in one pass both inspection and detailed structural assessment that minimally interfere with tunnel traffic (one-lane closure is required) [25]. Figure 3 depicts the final ROBO-SPECT robotic system.

The robotic system research and validation sites include the VSH infrastructure in Switzerland, London Underground tunnels, and Egnatia Motorway tunnels in Greece. The specific objectives of the robotic system are the following:

- Increase the speed and reliability of tunnel inspections.
- Provide assessment in addition to inspection.
- Minimize the use of scarce tunnel inspectors, while improving the working conditions of such inspectors.
- Decrease inspection and assessment costs.
- Increase the safety of passengers.
- Decrease the periods when tunnels are closed for inspection.

In summary, the needs which ROBO-SPECT addresses are the following [26]:

- Inspection, assessment and repair of the existing infrastructure are of utmost importance because of the high cost of new tunnel constructions.

- Transport demand is highly increasing, so a preventive maintenance to maximize the operational uptime of tunnels is fundamental.
- Inspection and assessment should be rapid in order to minimize tunnel closures or partial closures.
- Engineering hours for tunnel inspection and assessment are severely limited.
- Manual inspection of tunnels is a slow and labor intensive process in an unpleasant environment.
- To bring more reliable classification of the liner conditions and engineering analysis.

Figure 3: ROBO-SPECT is a research project co-funded by the European Commission under the FP7 ICT on Robotics use cases & Accompanying measures.

3. The ROBO-SPECT System Architecture and Integrated Components Design

The architecture of the ROBO-SPECT system is composed by three different integrated components that allow the comprehensive inspection and assessment of tunnels, aimed at providing the functionalities specified by the ROBO-SPECT end-users group [27]. The first component is the robotic system. The robotic system includes all the different sensors that are used during the inspection, and performs the inspection inside the tunnel. The second component is the Ground Control Station (GCS), which works as a central unit to prepare and monitor the robot missions (complete inspection sequences), and communicate with the platform. The GCS also works as a link between the robot and the third component, the Control Room (CR). The CR is equipped with the PCs that contain the Structural Assessment Tool. This software uses the inspection results to generate a complete assessment report about the tunnel state.

3.1. Robotic System

The ROBO-SPECT robotic system is composed of a robotized mobile vehicle capable of extending an automated crane to the dimensions commonly found in metro and motorway tunnels. In order to measure width and depth of detected cracks inside the tunnel, the robotic system is equipped with a specifically designed ultrasonic sensor (US) robotic tool and a robotic arm for positioning it with high accuracy. A set of computer vision cameras are used for detecting cracks and other defects on the tunnel lining, and a 3D laser profiler provides data to detect deformations of the tunnel through the assessment tool. An additional set of cameras are attached to the crane and an Internet Protocol (IP) camera is placed on the tip of the arm for an extra teleoperation mode. The actual design of the robotic system and its different components are depicted in Figure 4. The mechanical design of the system is based on the one used in the TUNCONSTRUCT European FP6 project [20], which used a similar vehicle, crane and robotic arm configuration.

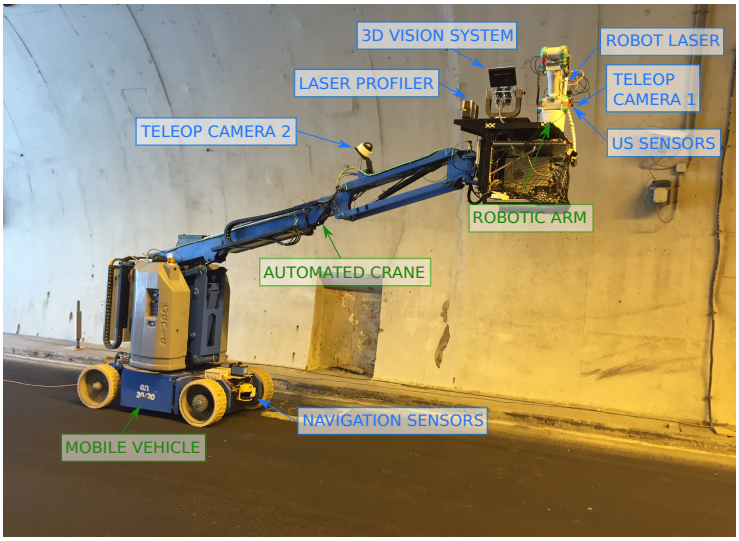

Figure 4: The ROBO-SPECT robotic system design includes: Mobile Vehicle, Automated Crane, Robotic Arm & Ultrasonic Sensors (US), Vision & Laser Profiler and Teleoperation Cameras.

3.1.1. Mobile Vehicle

The robotic platform is able to advance along the roadway tunnel to cover the applicability of the robotic system. This mobile vehicle navigates autonomously following tunnel lining at a constant distance and performs collision avoidance through the tunnel using front and back SICK S3000 range laser navigation sensors. The navigation strategy is based on Simultaneous Localization and Mapping (SLAM) using a set of reflective beacons placed inside the tunnel. Pairs of beacons are placed asymmetrically along the tunnel every 15 m. These beacons are detected by the NAV200 navigation sensor and are used to update the localization of the robot in the tunnel and simultaneously build a 2D map of the navigated section. This map can be used to improve navigation precision in successive inspections. Figure 5 depicts the Genie Z30/20N industrial robotic platform composed by the mobile vehicle and the automated crane.

Figure 5: ROBO-SPECT vehicle and crane.

3.1.2. Automated Crane

The crane has been sensorized through installation of angular and linear encoders in the joints in order to control the crane tip position and orientation. The joints of the system are also adapted with special absorbers to minimize the oscillation and vibration of the parts. The crane tip has been redesigned to carry a platform with the robotic arm equipped with the ultrasonic sensor, the set of cameras attached to a pan & tilt mechanism, and the 3D laser profiler. The crane can position the selected platform at a maximum height of 10 meters from the ground, which is adequate for the majority of roadway tunnels.

3.1.3. Robotic Arm

The high precision robotic arm placed on the crane platform is the Mitsubishi PA-10, a 7 Degree of Freedom (DoF) industrial manipulator. In order to provide the arm with full position and orientation capabilities, 6 DoF are required. The extra DoF adds redundancy to provide the robotic arm with obstacle avoidance and correct orientation capabilities. The effective workspace of the robot ranges from a few centimeters to 1 meter approximately from the base of the arm to the end-effector; which is, however, limited by basic kinematic singularities and self-collisions. The ultrasonic sensor is located at the tip of the robot. The

main mission of the robot is to place the ultrasonic sensor on cracks on the tunnel lining to perform width and depth measurements (Figure 6). In order to calculate a safe trajectory to the final point, a Hokuyo UBG-04LX-F01 2D range robot laser sensor is attached to a link of the arm to scan the surroundings of the crack position and create an online 3D point cloud of the tunnel lining before moving the system.

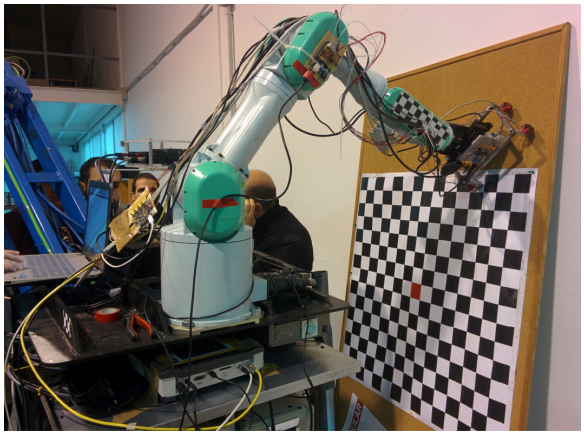

Figure 6: The 7 DoF robotic arm is able to safely position the ultrasonic sensor.

3.1.4. Vision System

The ROBO-SPECT vision system is composed by two pairs of Point Grey Grasshopper3 GS3-U3-91S6C-C 9.1 MP cameras to detect different defects on the tunnel lining during the inspection and an on-board lighting system to operate under proper lighting conditions. A pan & tilt mechanism designed to point these cameras is placed on the crane platform. It is important to highlight that the vision system needs to be positioned at a controlled distance to the wall, to maintain constant image resolution of millimeter accuracy. The first pair of cameras are designed to be able to identify a set of different defects commonly found in tunnels such as spalling, efflorescence and cracks. These defects are detected using deep learning based approaches. Convolutional Neural Networks (CNN) are trained with annotated data from real images of tunnel

defects [28]. Real-time 3D information is extracted to estimate the 3D positions and orientations of cracks. This data is then passed to the robot to move the crane to the crack surroundings first, and then move the robotic arm to touch the tunnel lining with the ultrasonic sensor. The second pair of cameras will be capable of taking a stereo image of the crack to be used later in the structural assessment tool for characterization purposes.

3.1.5. Laser Profiler

Furthermore, a Faro Focus3D X 130 3D laser profiler is placed on the crane platform in order to inspect tunnel structural deformation with an accuracy of ±2 mm. The chosen laser profiler provides points clouds to model the tunnel lining and measure the displacements of points with respect to their previous position due to deformation. Figure 7 depicts the vision system placed on the pan-tilt and the 3D laser profiler.

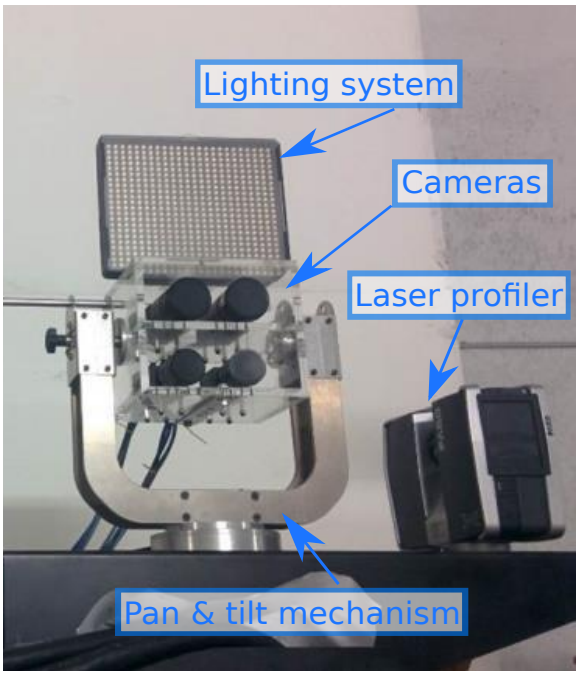

Figure 7: The ROBO-SPECT vision system and the 3D laser profiler are placed on the crane platform.

3.1.6. Ultrasonic Sensor (US)

At the tip of the robotic arm, an ultrasonic sensor is attached (Figure 8). This sensor is designed specifically for the ROBO-SPECT project to measure the width and depth of the crack while in contact with the tunnel lining. The depth measurement of the crack is computed applying the Time of Flight (ToF) detection method and performed using two James Instruments piezo-ceramic contact compression wave transducers with central frequency of 54 kHz [29]. Regarding the width measurement, a sliding contact tip sensor used to scan the concrete surface. The sensor has an additional XY translation mechanism for final positioning on the tunnel wall. When the system finishes taking the measurements, the robotic manipulator removes the sensors from the tunnel lining, and the inspection continues.

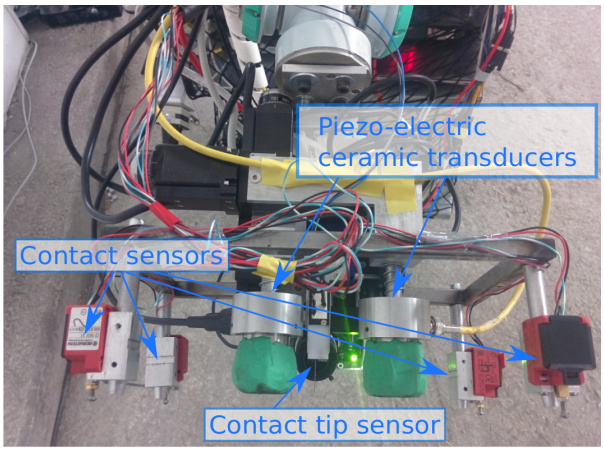

Figure 8: Ultrasonic sensor robotic tool to measure the width and depth of cracks is attached to the tip of the robotic arm.

3.1.7. Intelligent Global Controller (IGC)

The Intelligent Global Controller (IGC) assures coherent and optimized trajectories for the three different subsystems (the mobile vehicle, the automated crane, and the robotic arm). It commands the robot navigation through the tunnel, identifying when a crack has been detected, and commands the necessary crane and arm movements to place the ultrasonic sensor on the crack to

perform all the required measurements.

To avoid undesired latencies in the control of all the different subsystems, the IGC is placed within the mobile vehicle to manage communications between parts. The software used to communicate between them is based on Yet Another Robot Platform (YARP) [30] and Robot Operating System (ROS) [31] as seen in Figure 9. All the different components (mobile vehicle, crane, cameras, etc) are connected to a local area network to receive the commands from the IGC and provide measurements and their state.

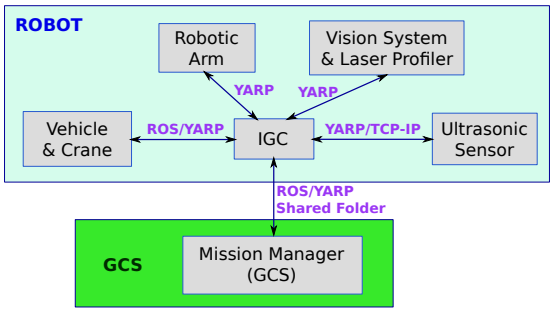

Figure 9: The Intelligent Global Controller (IGC) communicates with the different components of the system.

The IGC receives a mission from a Ground Control Station (GCS) and provides the protocol to command the system in order to perform the requested inspection mission autonomously. It, in turn, updates the GCS with the state of the mission and the inspection data gathered.

3.2. Ground Control Station (GCS)

The Ground Control Station is a computer component outside the robotic system that is in contact with it. The GCS provides a graphical user interface and it works as a Human-Machine Interface (HMI). From the GCS, the end-user can provide a mission to the robot and retrieve the state of the mission while the robotic system is inside the tunnel. The communication between the robotic system and the GCS is based on a wireless connection.

3.3. Control Room (CR)

The Control Room is the last component of the ROBO-SPECT tunnel inspection system. The CR represents the site where all the data gathered by the robot is processed. This processing is performed by its Structural Assessment Tool (SAT), a software created inside the project to store, graphically represent, and process the inspection data (Figure 10). The SAT allows the end-user to see the generated maps of the tunnel, the 3D slices computed by the laser profiler, information about the different cracks and other defects detected, and their position inside the tunnel. It uses all the data to produce a complete assessment report of the structural state of the system that are presented to the end-users. The SAT is also able to use information from multiple inspections of the same tunnel separated in time to study the rate of deformation of the lining or the evolution of the cracks and other defects.

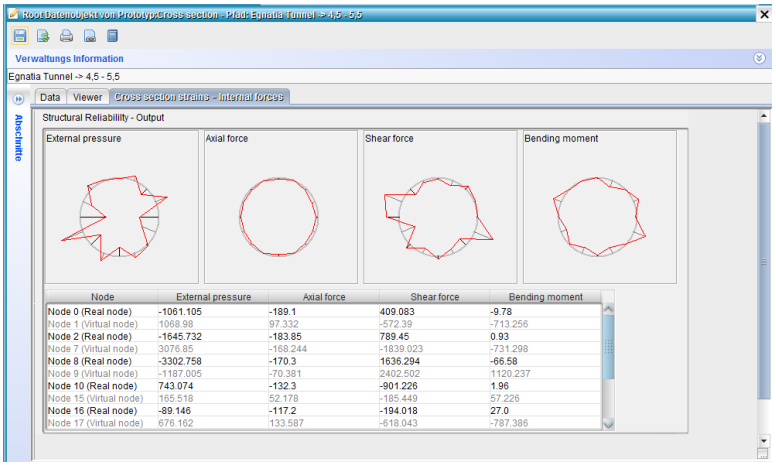

Figure 10: The Structural Assessment Tool (SAT) uses the inspection data to produce an assessment report.

The GCS is in contact with the CR as well, and depending on the tunnel and the end-user, the connection with the CR can be wireless, accessing the nearest access point of the infrastructure network or Internet, or a direct connection if the end-user processes the data once back in the company headquarters. This

communication provides the CR with all the inspection data gathered by the system to process later using the SAT.

4. Safe Positioning System of Ultrasonic Sensor (US)

Because a stable position of the ultrasonic sensor is needed while the measurements are taken, four contact sensors are placed on the corners of a rectangular frame attached to the tip of the robotic manipulator (Figure 8). These contact sensors, currently implemented as normally closed push switches, allow detecting the tunnel lining during the approach of the ultrasonic sensor. The safe positioning process is composed of four steps: arm creates surface map, move tip to a fixed distance from the surface, end-effector trajectory tracking control, and guided US normal approach and iterative rotation.

4.1. Arm creates surface map

In order to measure the width and depth of a crack, the arm must place the ultrasonic sensor (US) so that the crack is between the two piezo-electric ceramic transducers, and perpendicular to the straight line that connects their centers. For the computation of a safe trajectory to the final point, a 3D point cloud of the surroundings of the detected crack is extracted from the data obtained using the 2D range robot laser sensor attached to one of the robotic arm's links (Figure 11).

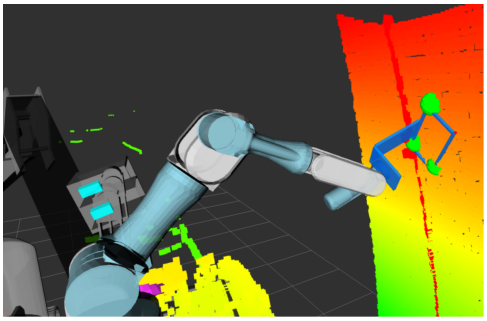

Figure 11: The 3D point cloud scan of the surroundings of the crack and the switches in contact are simultaneously visualized.

With the extracted 3D point cloud, the 3D normal to the tunnel lining on the crack position is computed. RRT-Connect planner [32] from the Open Motion Planning Library (OMPL) is used to generate a safe joint trajectory to position the ultrasonic sensor on the point on the normal at a fixed distance from the surface (Figure 12, top left). The generated trajectory is defined as a sequence of waypoints in the joint space q. Each waypoint contains joint angles q_d, time t and velocity $\dot{q}_d$. The control algorithm described in Section 4.2 is used to track the calculated trajectory.

After that, the tip of the robotic arm moves following the calculated normal to contact the switches with the surface. Since the tunnel lining is not a simple flat wall, it is not likely for the four switches to simultaneously enter in contact with it. Therefore, the contact of three switches at the same time is considered sufficient. If fewer switches were in contact, the position would not remain stable, so the tip would be reorientated by using the information from the contact sensors (Section 4.4). The end-effector control during the approach and reorientation will be described in Section 4.3.

4.2. Move tip to a fixed distance from the surface

The joint space trajectory tracking control used for the arm, consists of two feedback loops: the internal motor driver PI torque controller inner loop, and the velocity PI controller outer loop. The joint velocity command at time t $\dot{q}_{cmd} \in \mathbb{R}^n$ for the outer controller can be obtained by utilizing the following expression:

$$\boldsymbol{\dot{q}_{cmd} = \dot{q}_d + K(q_d - q)} \tag{1}$$

where $q_d \in \mathbb{R}^n$ and $\dot{q}_d \in \mathbb{R}^n$ are the joint angle and the joint velocity vectors at time t of the generated trajectory, $q \in \mathbb{R}^n$ is the current joint angle vector and $K \in \mathbb{R}^{n \times n}$ is a diagonal positive definitive matrix.

4.3. End-Effector Trajectory Tracking Control

Using the Resolved Motion Rate Control (RMRC) as a kinematic control [33], the desired joint velocity vector can be described as:

$$\dot{\boldsymbol{q}}_{\boldsymbol{d}} = \boldsymbol{J}(\boldsymbol{q})^{\dagger}(\dot{\boldsymbol{x}}_{\boldsymbol{d}} + \boldsymbol{K}(\boldsymbol{x}_{\boldsymbol{d}} - \boldsymbol{x})) \tag{2}$$

where $J(q)^{\dagger} \in \mathbb{R}^{n \times 6}$ is the right pseudoinverse of the robot's Jacobian matrix, $\dot{x}_d \in \mathbb{R}^6$ is the time derivative of the desired pose vector $x_d \in \mathbb{R}^6$, $x \in \mathbb{R}^6$ is the pose vector of the end-effector, and $K \in \mathbb{R}^{6 \times 6}$ is a symmetric positive definite matrix.

4.4. Guided US normal approach and iterative rotation

The guided approach and iterative rotation algorithm is based on the iterative change of the tip coordinate system and rotation during the motion described in Section 4.3 around each of its axes until the position is stable (Figure 12, bottom right). The process depends on which of the frame switches are in contact:

1. When one switch is in contact, the new coordinate system is placed there and the tip will rotate around one of the frame sides that meet on this corner (Figure 12, top right).
2. In case of two adjacent switches in contact, the new coordinate system is placed in the middle point of the straight line through them, and the tip will rotate around this line (Figure 12, bottom left).
3. Finally, when two diagonal switches are in contact, the new coordinate system will be the centre of the frame and it will rotate around the diagonal which links them. The algorithm will select clockwise or counter-clockwise rotation in order to obtain more switches in contact.

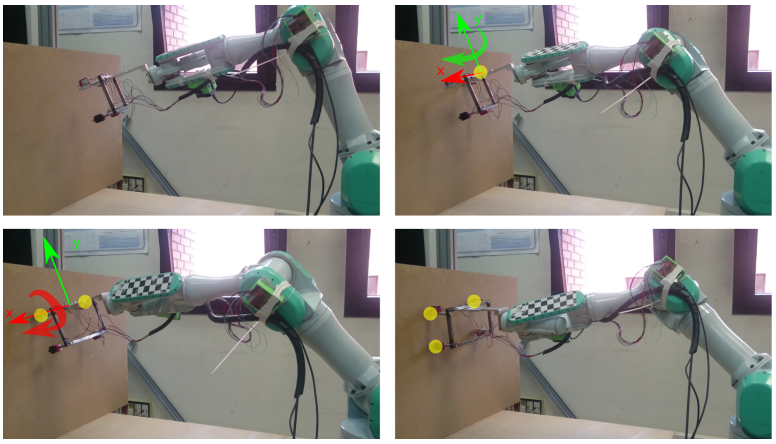

Figure 12: Sequences of the iterative rotation algorithm performed in the laboratory against a flat surface, with switches in contact depicted in yellow.

5. Laboratory and Field Experiments

The ROBO-SPECT system for robotic tunnel inspection has been successfully tested in a number of different settings, ranging from simulated environments to motorway roads with ongoing traffic flow.

- Initial experiments were performed within a Gazebo [34] simulated environment of the complete system. In contrast to other fields, robotic simulated environments represent the nature of unpredictable events rather faithfully. Robotic simulator collision detectors and physics engines tend to make them fit for testing algorithms which work with inexact models. These experiments served to validate the functionality of the US positioning algorithm.

- The robotic arm without the crane and with the sensor tip system was then tested in laboratory settings, using mock objects to simulate the tunnel intrados. These experiments served to take into account the physical elements related to the system, such as the importance of the robustness of the contact sensors, and the role the positioning system duration can play in proportion to the full tunnel inspection procedure time.

- The full robotic system was tested in Valencia, mounting the robotic arm on the crane and robotic vehicle, together with the complete tunnel inspection equipment, also in laboratory settings. These experiments served for further hardware integration, and improvements in YARP [30] and ROS [31] software communication protocols.

- The full robotic system was tested in Metsovo, Greece, in Egnatia Odos motorway tunnels with and without ongoing traffic. Figure 13 depicts trials in the Metsovo Malakasi Tunnel, of 10 m diameter and 7 m height. Roadway tunnel experiments were performed throughout different validation scenarios, including all parts of the inspection process. Mission plans were sent to the IGC using the GCS Mission Manager without human intervention. The GCS was connected to the CR, where the data gathered on these experiments was monitored in real time. The first scenario consisted of image acquisition every 1.4 m half-slice of the tunnel. The second scenario was the same as the first one, but with added 3D laser profiler scans every 5 m. The third scenario consisted of image acquisition and crack detection without approaching to the the tunnel lining every 1.4 m, and 3D laser profiler scans every 5 m. The fourth scenario included image acquisition, crack detection, stereo images acquisition, 3D laser profiler scans if a crack is detected in the segment and other defects detection algorithms at the end of the inspection. The fifth scenario added the teleoperation mode of the robotic arm to place the US sensor tool on detected cracks to perform width and depth measurements. The last scenario demonstrated the comprehensive autonomous inspection procedure developed in the ROBO-SPECT project with all the processes performed autonomously, from which the final results were collected.

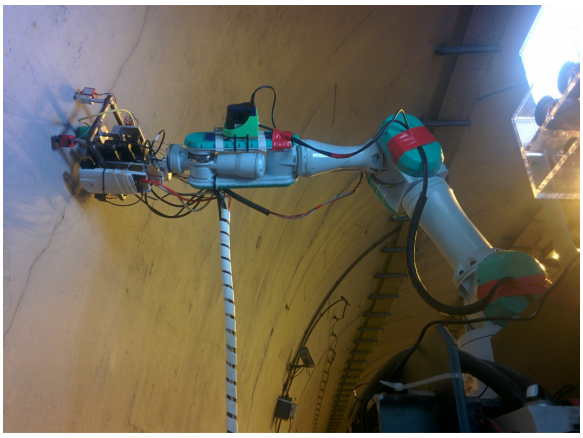

Figure 13: Ultrasonic sensors touching a detected crack inside the Metsovo Malakasi tunnel.

6. Experimental Results

The comprehensive autonomous inspection procedure developed in the ROBO-SPECT project consists of a slice by slice inspection, where a complete half of the tunnel is inspected in one pass, and the other half of the tunnel can be inspected on a returning pass. Given the camera resolution, the slice width of robotic inspection is set to 1.4 m to assure the 1 mm precision. When it is finished, it stores the data and advances to analyze the next slice. The crane movement is minimized, e.g. down to two different positions for camera crack detection of a half-slice in the Metsovo Tunnel, using the pan & tilt mechanism to orient cameras for inspection. If one crack is detected by the computer vision system, the crane has to approach the tunnel lining so the robotic arm moves to touch the surface with the US on the crack (Figure 14).

After the measurements are taken, the crane returns to its home position and a laser profiler scan of the slice is performed.

From the field experiments at Egnatia Tunnel on June and July 2016, timing and accuracy data of inspection process was gathered. 10 full trials of the final comprehensive autonomous inspection procedure were performed on a 20 m tunnel segment. These 20 m correspond to 15 slices, where the extra 1 m corresponds to overlapping images for mosaic matching and stitching.

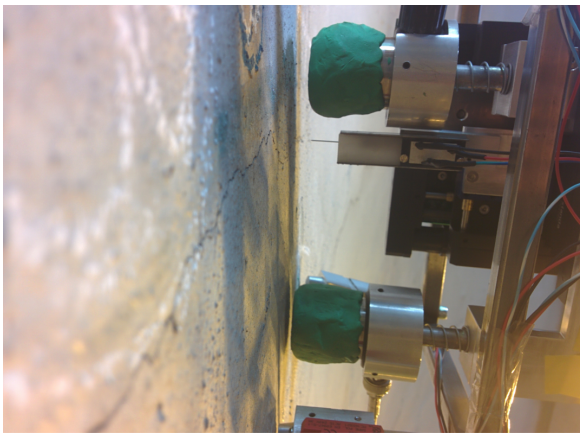

Figure 14: Closer view of the US sensors measuring a crack inside the Metsovo Malakasi Tunnel.

Regarding the inspection by computer vision, images were evaluated through the defect detector and classified in cracks (positive) and non-cracks (negative). Given the number of true positives, false positives, true negatives and false negatives, several performance metrics were calculated. The defect detection algorithm has demonstrated a sensitivity of 0.8981, a miss rate of 0.1019, and an accuracy of 0.8684. Figure 15 depicts sample results of the crack detection and reconstruction algorithms. Further details on the computer vision system are available in [35].

In terms of the ultrasonic sensor, the agreement between the automated system and independent manually performed width measurements was 0.1 mm. The ultrasonic sensor was tested on concrete mock-ups with artificial cracks, performing crack depth measurements with a relative accuracy of 5% [29]. Manual measurements were gathered using ultrasonic sensors with an ultrasound gel to improve ultrasonic transmission on concrete, which was not used in the automated system.

Experimental results related with times and precisions of the robotic part of the system are presented in Section 6.1 and 6.2 respectively.

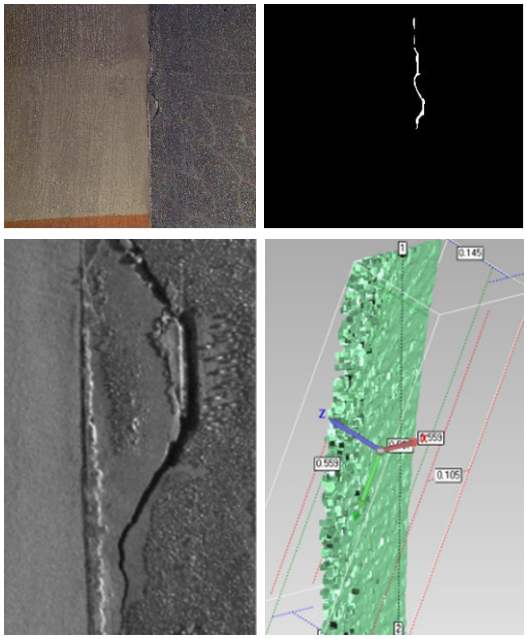

Figure 15: Example of the crack detection and stereo reconstruction results. In the first row, left image of a stereo-pair on the Egnatia tunnel and the detected crack are shown. The second row depicts a detail of the left image and the isometric projective view of the 3D reconstruction model generated around the detected crack.

6.1. Inspection process timing

The final result for the 20 m tunnel segment inspection timing is 2 hours and 9 minutes. The inspected tunnel presents a two to three ratio of cracks per half-slice, which implies there were five half-slices without cracks, and ten half-slices with cracks that were consistently detected by the vision system. Table 1 depicts the average time of each inspection process stage extracted from the trials.

The total time to inspect one 1.4 m half-slice of the tunnel without cracks (approximately 6 minutes) is highlighted in this Table after the set of stages that are required for this process. The total time to inspect one 1.4 m half-slice of the tunnel with one crack (less than 10 minutes) is highlighted in the same Table after the set of stages that are additionally required. Manual in-

spection of one crack in the same tunnel by two operators at a maximum 1.5 m height was measured to take between 15 and 16 minutes, which is over 5 minutes more than with the ROBO-SPECT robotic system. At larger heights greater than 1.5 m, manual inspection takes considerably more time, since operators require mounting on a manually controlled crane or colossus scaffolds. The measurement time of less than 10 minutes presented in this paper is an improvement with respect to the robotic system for tunnel inspection of [20], in which the manually controlled crane took near half an hour for positioning and stabilization.

Table 1: Inspection process timing of one 1.4 m half-slice measured in Egnatia tunnel on June and July 2016.

Inspection Process Stages	Time [s]
Vehicle motion to next 1.4 m slice	10
Crane motion to first scanning position	21
Crane stabilization	4
Crack detection in first position	150
Crane motion to second scanning position	35
Crane stabilization	4
Crack detection in second position	120
Crane go to home position	26
Inspect one half-slice without cracks	**370**
Crane approach to the wall	7
Robotic arm tip touch the wall	15
US Measurements	80
Laser profiler scanning	120
Inspect one half-slice with one crack	**592**

6.2. Inspection process precision

The overall precision of the ROBO-SPECT system describes the precision of the US positioning on a given crack with respect to the global tunnel coordinates. The coordinates ground truth is based on a previously hand-crafted map of tunnel lining cracks.

The overall precision is shown together with each ROBO-SPECT individual component average precision in Table 2. For the complete ROBO-SPECT system, the overall maximum error is 11 cm. This value reflects the accumulated

errors from the chain starting with the vehicle position, passing through the crane encoders, computer vision system, robot laser sensor, robotic arm, and ending at the ultrasonic sensors.

Table 2: Precision of each ROBO-SPECT component, and the maximum accumulated error from the chain that begins with the vehicle position and ends with the US placement.

	Average precision	
Component	Pos. [mm]	Or. [°]
Vehicle	25	0.06
Crane	30	0.22
Vision system	10	0.35
Robot laser sensor	2	0.01
Robotic arm	3	0.01
Ultrasonic Sensors	1	0.05

	Maximum error	
Component	Pos. [mm]	Or. [°]
Vehicle	38	0.10
Crane	47	0.34
Vision system	16	0.55
Robot laser sensor	3	0.02
Robotic arm	4	0.02
Ultrasonic sensors	2	0.07

	Maximum error	
Chain	Pos. [mm]	Or. [°]
Vehicle	38	0.10
Veh. + Crane	85	0.44
Veh. + Crane + Vis.	101	0.99
Veh. + Crane + Vis. + Laser	104	1.01
Veh. + Crane + Vis. + Laser + Arm	108	1.03
Veh. + Crane + Vis. + Laser + Arm + US	**110**	**1.10**

7. Conclusions

ROBO-SPECT is a highly complex system capable of inspecting roadway tunnels autonomously without compromising the safety of operators and with ongoing traffic on the other lane of the roadway. The system has robustly performed full inspection, with end-users only monitoring the process during the numerous field testings. The mobile vehicle has demonstrated its ability to navigate autonomously through real tunnels using the reflective beacons system and

the dedicated laser navigation sensors while avoiding obstacles and maintaining a constant parametrized distance to the wall. The automated crane performed trajectory plans with collision avoidance using a 3D point cloud map. The robotic arm successfully placed the ultrasonic sensors with precision on the tunnel lining.

The integrated mode of operation, where the three levels (robotic system, GCS and Control room) are connected permanently was tested positively detecting cracks and gathering images and US measurements, finally displayed through the SAT. A large number of mechanical, hardware and software adaptations allowed the overall system integration in a positive way. The software integration, including IGC and GCS, shows that the chosen architecture and protocols perform correctly, including non-standard situations.

The ROBO-SPECT robotic system provides accurate, faster and reliable tunnel lining inspection and assessment with ongoing traffic in safer working conditions.

Acknowledgements

This work was supported by ROBO-SPECT project number 611145 co-funded by the European Commission under 7th Framework program, RoboCity2030-II-CM project (S2009/DPI-1559) funded by Programas de Actividades I+D in Comunidad de Madrid and co-funded by Structural Funds of the EU, and ARCADIA project DPI2010-21047-C02-01 funded by CICYT project grant.

References

[1] W. Bergeson, S. Ernst, Tunnel Operations, Maintenance, Inspection and Evaluation (TOMIE) Manual, Transportation Research Board of the National Academies, 2015.
http://dx.doi.org/10.3141/2592-18

[2] A. Haack, Current safety issues in traffic tunnels, Tunnelling and underground space technology 17 (2) (2002) 117–127.
http://dx.doi.org/10.1016/S0886-7798(02)00013-5

[3] C. Balaguer, R. Montero, J. Victores, S. Martínez, A. Jardón, Towards fully automated tunnel inspection: A survey and future trends, in: ISARC. Proceedings of the International Symposium on Automation and Robotics in Construction, Vol. 31, 2014, pp. 19–33.
http://dx.doi.org/10.22260/ISARC2014/0005

[4] A. Wimsatt, J. White, C. Leung, T. Scullion, S. Hurlebaus, D. Zollinger, Z. Grasley, S. Nazarian, H. Azari, D. Yuan, et al., Mapping voids, debonding, delaminations, moisture, and other defects behind or within tunnel linings, SHRP 2 Report S2-R06G-RR-1, The National Academies Press, 2014.
http://dx.doi.org/10.17226/22609

[5] Y. Shen, B. Gao, X. Yang, S. Tao, Seismic damage mechanism and dynamic deformation characteristic analysis of mountain tunnel after wenchuan earthquake, Engineering Geology 180 (2014) 85–98.
http://dx.doi.org/10.1016/j.enggeo.2014.07.017

[6] A. Bin Ibrahim, P. Bin Ismail, M. Forde, R. Gilmour, K. Kato, A. Khan, N. Ooka, S. Siong, K. Terada, H. Wiggenhauser, Guide book on non-destructive testing of concrete structures, 2002, (ISSN:10185518).

[7] D. Liberatore, N. Masini, L. Sorrentino, V. Racina, M. Sileo, O. AlShawa, L. Frezza, Static penetration test for historical masonry mortar, Construction and Building Materials 122 (2016) 810–822.
http://dx.doi.org/10.1016/j.conbuildmat.2016.07.097

[8] A. Basu, A. Aydin, A method for normalization of schmidt hammer rebound values, International journal of rock mechanics and mining sciences 41 (7) (2004) 1211–1214.
http://dx.doi.org/10.1016/j.ijrmms.2004.05.001

[9] N. Gucunski, et al., Nondestructive testing to identify concrete bridge deck deterioration, Transportation Research Board, 2013.
http://dx.doi.org/10.17226/22771

[10] H. Toutanji, Ultrasonic wave velocity signal interpretation of simulated concrete bridge decks, Materials and Structures 33 (3) (2000) 207–215.
http://dx.doi.org/10.1007/BF02479416

[11] J. Makar, R. Desnoyers, Magnetic field techniques for the inspection of steel under concrete cover, NDT & e International 34 (7) (2001) 445–456.
http://dx.doi.org/10.1016/S0963-8695(00)00051-7

[12] R. B. Polder, Test methods for on site measurement of resistivity of concrete – a RILEM TC-154 technical recommendation, Construction and building materials 15 (2) (2001) 125–131.
http://dx.doi.org/10.1016/S0950-0618(00)00061-1

[13] D. Wu, G. Busse, Lock-in thermography for nondestructive evaluation of materials, Revue générale de thermique 37 (8) (1998) 693–703.
http://dx.doi.org/10.1016/S0035-3159(98)80047-0

[14] G. Parkinson, C. Ékes, Ground penetrating radar evaluation of concrete tunnel linings, in: 12th International Conference on Ground Penetrating Radar. Birmingham, UK, 2008, p. 11, (ISBN: 0956112102).

[15] O. Büyüköztürk, Imaging of concrete structures, Ndt & E International 31 (4) (1998) 233–243.
http://dx.doi.org/10.1016/S0963-8695(98)00012-7

[16] S.-N. Yu, J.-H. Jang, C.-S. Han, Auto inspection system using a mobile robot for detecting concrete cracks in a tunnel, Automation in Construction 16 (3) (2007) 255 – 261.
http://dx.doi.org/10.1016/j.autcon.2006.05.003

[17] F. Yao, G. Shao, R. Takaue, A. Tamaki, Automatic concrete tunnel inspection robot system, Advanced Robotics 17 (4) (2003) 319–337.
http://dx.doi.org/10.1163/156855303765203029

[18] T. Suda, A. Tabata, J. Kawakami, T. Suzuki, Development of an impact sound diagnosis system for tunnel concrete lining, in: Tunneling and Underground Space Technology. Underground Space for Sustainable Urban Development. Proceedings of the 30th ITA-AITES World Tunnel Congress Singapore,22-27 May 2004, Vol. 19, 2004, pp. 328–329.
http://dx.doi.org/10.1016/j.tust.2004.01.026

[19] J. H. Lee, J. M. Lee, J. W. Park, Y. S. Moon, Efficient algorithms for automatic detection of cracks on a concrete bridge, in: ITC-CSCC: International Technical Conference on Circuits Systems, Computers and Communications, 2008, pp. 1213–1216, (ISBN: 978-4-88552-233-8 C3055).

[20] J.G. Victores, S. Martínez, A. Jardón, C. Balaguer, Robot-aided tunnel inspection and maintenance system by vision and proximity sensor integration, Automation in Construction 20 (5) (2011) 629–636.
http://dx.doi.org/10.1016/j.autcon.2010.12.005

[21] H. M. La, N. Gucunski, S.-H. Kee, J. Yi, T. Senlet, L. Nguyen, Autonomous robotic system for bridge deck data collection and analysis, in: Intelligent Robots and Systems (IROS 2014), 2014 IEEE/RSJ International Conference on, IEEE, 2014, pp. 1950–1955.
http://dx.doi.org/10.1109/iros.2014.6942821

[22] H. M. La, N. Gucunski, K. Dana, S.-H. Kee, Development of an autonomous bridge deck inspection robotic system, Journal of Field Robotics (2017) 1–16.
http://dx.doi.org/10.1002/rob.21725

[23] P. Prasanna, K. J. Dana, N. Gucunski, B. B. Basily, H. M. La, R. S. Lim, H. Parvardeh, Automated crack detection on concrete bridges, IEEE

Transactions on Automation Science and Engineering 13 (2) (2016) 591–599.
http://dx.doi.org/10.1109/tase.2014.2354314

[24] N. Gucunski, S.-H. Kee, H. La, B. Basily, A. Maher, Delamination and concrete quality assessment of concrete bridge decks using a fully autonomous rabit platform, International Journal of Structural Monitoring and Maintenance 2 (1) (2015) 19–34.
http://dx.doi.org/10.12989/smm.2015.2.1.019

[25] R. Montero, J.G. Victores, S. Martínez, A. Jardón, C. Balaguer, Past, present and future of robotic tunnel inspection, Automation in Construction 59 (2015) 99–112.
http://dx.doi.org/10.1016/j.autcon.2015.02.003

[26] K. Loupos, A. Amditis, C. Stentoumis, P. Chrobocinski, J.G. Victores, M. Wietek, P. Panetsos, A. Roncaglia, S. Camarinopoulos, V. Kalidromitis, et al., Robotic intelligent vision and control for tunnel inspection and evaluation-the robinspect ec project, in: Robotic and Sensors Environments (ROSE), 2014 IEEE International Symposium on, IEEE, 2014, pp. 72–77.
http://dx.doi.org/10.1109/ROSE.2014.6952986

[27] R. Montero, J.G. Victores, E. Menendez, C. Balaguer, The robot-spect eu project: Autonomous robotic tunnel inspection, in: Robocity2030 13th Workshop EU robotic projects results, 2015, pp. 91 – 100, (ISBN: 978-84-608-4160-9).

[28] K. Makantasis, E. Protopapadakis, A. Doulamis, N. Doulamis, C. Loupos, Deep convolutional neural networks for efficient vision based tunnel inspection, in: 2015 IEEE International Conference on Intelligent Computer Communication and Processing (ICCP), IEEE, 2015, pp. 335–342.
http://dx.doi.org/10.1109/ICCP.2015.7312681

[29] L. Belsito, L. Masini, M. Sanmartin, K. Loupos, A. Roncaglia, Ultrasonic sensor system for automatic depth measurement of surface opening cracks

in concrete by means of a robotic arm, in: Transforming the Future of Infrastructure through Smarter Information: Proceedings of the International Conference on Smart Infrastructure and Construction, 2016, pp. 239–244, (ISBN: 978-0-7277-6127-9).

[30] G. Metta, P. Fitzpatrick, L. Natale, Yarp: yet another robot platform, International Journal on Advanced Robotics Systems 3 (1) (2006) 43–48. http://dx.doi.org/10.5772/5761

[31] M. Quigley, K. Conley, B. Gerkey, J. Faust, T. Foote, J. Leibs, R. Wheeler, A. Y. Ng, ROS: an open-source Robot Operating System, in: ICRA workshop on open source software, Vol. 3, Kobe, Japan, 2009, p. 5, Available at https://www.willowgarage.com/sites/default/files/icraoss09-ROS.pdf [Accessed 28 11 2017].

[32] J. J. Kuffner, S. M. LaValle, Rrt-connect: An efficient approach to single-query path planning, in: Robotics and Automation, 2000. Proceedings. ICRA'00. IEEE International Conference on, Vol. 2, IEEE, 2000, pp. 995–1001.
http://dx.doi.org/10.1109/ROBOT.2000.844730

[33] R. Kelly, J. Moreno, Manipulator motion control in operational space using joint velocity inner loops, Automatica 41 (8) (2005) 1423–1432.
http://dx.doi.org/10.1016/j.automatica.2005.03.008

[34] B. Gerkey, R. T. Vaughan, A. Howard, The player/stage project: Tools for multi-robot and distributed sensor systems, in: Proceedings of the 11th international conference on advanced robotics, Vol. 1, 2003, pp. 317–323, (ISBN: 9729688982).

[35] E. Protopapadakis, K. Makantasis, G. Kopsiaftis, N. Doulamis, A. Amditis, Crack identification via user feedback, convolutional neural networks and laser scanners for tunnel infrastructures, in: Proceedings of the 11th Joint Conference on Computer Vision, Imaging and Computer Graphics Theory

and Applications (VISIGRAPP 2016), Vol. 4, 2016, pp. 725–734, (ISBN: 978-989-758-175-5).
http://dx.doi.org/10.5220/0005853007250734